



# Enhanced Electrochemical Performance of Electropolymerized Self-Organized TiO<sub>2</sub> Nanotubes Fabricated by Anodization of Ti Grid

Vinsensia Ade Sugiawati<sup>1</sup>, Florence Vacandio<sup>2</sup>, Alina Galeyeva<sup>3</sup>, Andrey P. Kurbatov<sup>3</sup> and Thierry Djenizian<sup>1\*</sup>

<sup>1</sup> Mines Saint-Etienne, Center of Microelectronics in Provence, Department of Flexible Electronics, Gardanne, France, <sup>2</sup> Aix Marseille Université, CNRS, Electrochemistry of Materials Research Group, MADIREL, UMR 7246, Marseille, France, <sup>3</sup> Center of Physical-Chemical Methods of Research and Analysis, Al-Farabi Kazakh National University, Almaty, Kazakhstan

## OPEN ACCESS

### Edited by:

Vardan Galstyan,  
University of Brescia, Italy

### Reviewed by:

Jan M. Macak,  
University of Pardubice, Czechia  
Giuseppe Barillaro,  
University of Pisa, Italy

### \*Correspondence:

Thierry Djenizian  
thierry.djenizian@emse.fr

### Specialty section:

This article was submitted to  
Physical Chemistry and Chemical  
Physics,  
a section of the journal  
Frontiers in Physics

Received: 05 September 2019

Accepted: 22 October 2019

Published: 12 November 2019

### Citation:

Sugiawati VA, Vacandio F, Galeyeva A,  
Kurbatov AP and Djenizian T (2019)  
Enhanced Electrochemical  
Performance of Electropolymerized  
Self-Organized TiO<sub>2</sub> Nanotubes  
Fabricated by Anodization of Ti Grid.  
Front. Phys. 7:179.  
doi: 10.3389/fphy.2019.00179

Self-organized Titanium dioxide (TiO<sub>2</sub>) nanotubes grown on Ti grid acting as anode for Li-ion microbatteries were prepared via an electrochemical anodization. By tuning the anodization time, the morphology and length of the nanotubes were investigated by scanning electron microscope. When the anodization time reached 1.5 h, the TiO<sub>2</sub>nts/Ti grid anode showed a well-defined nanotubes, which are stable, well-adherent ~90 nm with a length of 1.9 ± 0.1 μm. Due to their high surface utilization, surface area, and material loading per unit area, TiO<sub>2</sub>nts/Ti grid anode using polymer electrolyte exhibited a high areal capacity of 376 μAh cm<sup>-2</sup> at C/10 rate and a stable discharge plateau at 1.8 V without using a polymer binder and conductive additive. The storage capacity of the TiO<sub>2</sub>nts/Ti grid after 10 cycles is 15 times higher compared to previous reports using planar Ti foils.

**Keywords:** anode, microbatteries, polymer electrolyte, Ti grid, TiO<sub>2</sub> nanotubes

## INTRODUCTION

Due to their high energy density, no memory effect and long cycle life, rechargeable Li-ion batteries (LIBs) have been extensively used as power sources for many electronic devices [1–4]. More recently, all-solid-state microbatteries have attracted intense attention for powering miniaturized electronics such as wireless sensors and a wide range of applications for the Internet of Things (IoT) [5–8]. Titanium dioxide (TiO<sub>2</sub>) is an attractive and versatile material that is used in many technologies due to its unique properties such as high surface area, electronic properties, biocompatibility, and environmental well-being [9, 10]. Particularly, synthesis of nanostructured TiO<sub>2</sub> such as nanotubes, nanowires, and nanofibers has raised interest lately compared to the conventional microstructures due to their high surface-to-volume ratio [11–13]. The first reports on the formation of self-organized nanotubes on titanium by Assefpour-Dezfuly et al. [14] where Ti metal was firstly etched in alkaline peroxide, then anodized in chromic acid and later by Zwilling et al. [15] reported on the formation of nanoporous anodized TiO<sub>2</sub> nanotubes in a fluoride containing electrolyte. Since then, TiO<sub>2</sub> nanotubes have been extensively explored in various fields, such as photocatalysis [16], sensors [17], dye sensitized solar cells (DSSCs) [18], and energy storage device [19].

Various approaches, such as sol-gel, hydrothermal treatment, template assisted method, electrospinning, and electrochemical anodization have been employed to prepare one-dimensional TiO<sub>2</sub> nanostructures [20]. However, self-organized TiO<sub>2</sub>nts formed by anodization method is preferred owing to their simplicity, better control over the nanotube morphology and low-cost [19, 21]. Thus, pristine as well as chemically modified TiO<sub>2</sub>nts obtained by anodization have been used as negative electrodes for high performance LIBs [22–24]. Most studies on self-organized TiO<sub>2</sub>nts are focused on the planar surface, for instance Ti foil. The utilization of Ti grid as the substrate to synthesize the TiO<sub>2</sub>nts has been extensively studied owing to its flexibility and unique geometry [25, 26]. Much attentions have been paid on the fabrication of the TiO<sub>2</sub>nts on Ti grid as photoanode, possessing an enhanced performance in terms of photon absorption and electron collection efficiency compared to anodized Ti foil [27–29]. Previous studies have shown the use of TiO<sub>2</sub>nts/Ti grid in DSSCs can effectively improve the charge collection efficiency of ~3.15% [27]. Liu et al. fabricated vertically oriented TiO<sub>2</sub> nanotube arrays with controllable lengths on Ti grids by electrochemical anodization in ethylene glycol-based electrolyte and investigated their potential application as flexible electrodes for DSSCs [30]. The work reported by Motola et al. showed a high photocatalytic, antimicrobial and antibiofilm activities of the TiO<sub>2</sub> nanotube layers grown on Ti grid [31, 32].

Despite a large number of reports published on the fabrication of self-organized TiO<sub>2</sub>nts and their applications, the use of TiO<sub>2</sub>nts/Ti grid as anode material has never been investigated with a polymer electrolyte to achieve the fabrication of all-solid-state microbatteries. To improve the performance of the TiO<sub>2</sub>nts anodes for Li-ion microbatteries, self-organized TiO<sub>2</sub>nts grown on Ti grid is considered as a great choice owing to its large aspect ratio of length to diameter, higher surface area, and high Ti conversion into TiO<sub>2</sub>nts [33, 34]. Hence, the self-organized TiO<sub>2</sub>nts anode provides more easily access for the Li ions, which improves the electrochemical performance of the microbatteries. Herein, we report the fabrication of a liquid-free microbattery using self-organized TiO<sub>2</sub>nts/Ti grid filled by an electropolymerized electrolyte. The effect of the anodic oxidation time on the formation of the TiO<sub>2</sub>nts were investigated by scanning electron microscopy (SEM) and the electrochemical performances of the electropolymerized TiO<sub>2</sub>nts was also studied by cyclic voltammetry and galvanostatic charge/discharge cycling. Compared to planar Ti surfaces (i.e., foil and thin film), we confirm that the discharge capacity values obtained from TiO<sub>2</sub>nts supported on a Ti grid are strongly enhanced.

## EXPERIMENTAL

### Synthesis of TiO<sub>2</sub> Nanotubes

The TiO<sub>2</sub>nts anodes were fabricated by the electrochemical anodization of a titanium grid (Good Fellow 0.57 mm thickness, 0.23 mm wire diameter). Before anodization, the Ti grids were cut to 1.3 × 1.3 cm<sup>2</sup> in size and cleaned via sonication in acetone, isopropanol, and methanol for 10 min each in order to remove any surface impurity. After drying the grids with compressed air, TiO<sub>2</sub>nts were grown by the anodization of Ti grid in an

organic electrolyte containing 96.7 wt. % glycerol, 1.3 wt. % NH<sub>4</sub>F, and 2 wt. % water [35]. All the anodization experiments were carried out at room temperature in a two-electrode system with a Ti grid as a working electrode and platinum (Pt) foil as a counter electrode. The working electrode was pressed against an O-ring of the electrochemical cell leaving ~0.63 cm<sup>2</sup> exposed to the electrolyte. The distance between the working and counter electrodes was set to 2 cm and the anodization was performed at room temperature without stirring of the electrolyte during anodization. A constant voltage of 60 V was applied to the two-electrode electrochemical cell using a generator (ISO-TECH IPS-603) for 1, 1.5, 2.5, and 3 h, respectively. After anodization, the samples were dipped in 0.5 vol. % HF solution for 30 s in order to remove the residue of the electrolyte, washed with distilled water and dried using compressed air. The as-formed TiO<sub>2</sub>nts were annealed at 450°C in air for 3 h with a heating rate of 5°C min<sup>-1</sup> in order to obtain anatase phase.

### Electrochemical Polymerization

In order to achieve the electrodeposition of PMMA-PEG (poly methyl ether methacrylate-polyethylene glycol) polymer electrolyte, cyclic voltammetry was performed on the TiO<sub>2</sub>nts in a three-electrode system using a VersaSTAT 3 potentiostat (Princeton Applied Research), Ag/AgCl as the reference and Pt electrode as the counter electrode in an aqueous solution composed of 0.5 M of bis(trifluoromethanesulfone)imide (LiTFSI) and 0.5 M MMA-PEG (methyl ether methacrylate-polyethylene glycol) with an average molecular weight of 500 g mol<sup>-1</sup>. Prior to electropolymerization, the aqueous solution containing the polymer electrolyte was purged with Argon gas for 10 min to remove dissolved oxygen. The cyclic voltammetry experiments were carried out for 100 cycles at the scan rate of 10 mV s<sup>-1</sup> in the potential window of -0.35 to -1 V vs. Ag/AgCl (saturated) [20, 36].

### Characterizations

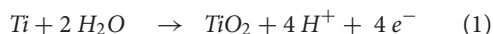
The crystallinity of the synthesized samples was examined by X-ray diffraction (XRD). The XRD pattern was recorded at room temperature using a Siemens D5000 diffractometer equipped with copper anticathode (Cu K<sub>α</sub> radiation of 0.1506 nm wavelength) was used with graphite monochromator). The diffractograms were analyzed by comparing with the JCPDS-ICDD database (Joint Committee on Powder Diffraction Standards International Center for Diffraction Data). The morphology of TiO<sub>2</sub>nts was investigated by SEM using a Carl Zeiss AG - ULTRA 55 SEM using an electron beam energy of 15 kV. The chronoamperometric test took place in a two-electrode electrochemical cell with Ti grid and Pt foil as a working and counter electrode, respectively, using PARSTAT 2273.

The Swagelok test cells were assembled in an Ar-filled glove box. In the half-cell system, TiO<sub>2</sub>nts electrodes were assembled against metallic Li foil using the gel electrolyte of the LiTFSI and MMA-PEG. The Li foil was cut in a circular shape with the diameter of 9 mm and 2 circular sheets (10 mm in diameter) of the gel electrolyte in the Whatman paper were used as separator. The cells were galvanostatically charged and discharged in the potential window of 1–3 V vs. Li/Li<sup>+</sup> at different current densities

and cyclic voltammetry was performed at a scan rate of 0.1 mV s<sup>-1</sup> using a VMP3 potentiostat-galvanostat (Bio Logic).

## RESULTS AND DISCUSSION

In this work, the growth of TiO<sub>2</sub> nanotubes was carried out by a low-cost and simple electrochemical anodization of Ti grid at different anodization time in a glycerol electrolyte containing fluoride ions and small amounts of water. **Figure 1A** shows the actual size of Ti grid used in the experiments and the inset shows the SEM image of the Ti grid. It can be seen Ti grid consist of many thin and radial Ti filaments which increase the surface area of the substrate. **Figure 1B** shows the chronoamperometric curve of Ti grid anodized at 60 V for 3 h. As seen, after a minor increase at the beginning of the anodization, the current density dropped with time due to the presence of an electrical barrier formed by the compact oxide layer. The minor increase in current density at the early stage of anodization might be attributed to the exposure of surface area that was not covered with the electrolyte due to the nature of the Ti grid structure. Self-organized TiO<sub>2</sub>nts starts to form as the result of the competition between electrochemical oxide formation and chemical dissolution of the oxide layer by fluoride ions according to Equations (1) and (2), respectively. Finally, steady current density was achieved when equilibrium was established between the growth and dissolution of the oxide layers [11].



The crystallinity of the TiO<sub>2</sub>nts was examined by XRD, as represented in **Figure 1C**. Immediately after growth the TiO<sub>2</sub>nts the tubes are amorphous and the formation of the anatase phase is obtained after annealing treatment. The presence of new peaks at about 25.3° and 47.9° correspond to the reflections of anatase phase (JCPDS file no. 21-1272). The Ti peaks observed on the XRD analysis are Ti substrate due to the direct growth of TiO<sub>2</sub>nts on the Ti grid. The residual Ti grid is directly used as the current collector.

In this work, effects of anodization time on the formation of TiO<sub>2</sub>nts arrays have been investigated. **Figures 2A–D** illustrates how the morphology and length of the anodized layer evolve with the anodizing time. The SEM images show the top surface and cross-section morphologies of TiO<sub>2</sub>nts anodized at 60 V for different durations of 1, 1.5, 2.5, and 3 h, respectively.

As seen, some changes can be observed with the increasing anodization time. For the shortest duration (1 h), the nanotubes are clearly visible and the length of the nanotubes is ca. 1.75 ± 0.1 μm (**Figure 2A**). However, the nanotube tops are not enough homogenous and smooth to ensure the conformal deposition of the polymer electrolyte. In **Figure 2B**, the SEM images showed the nanotubes anodized for 1.5 h has an open-top structure without any bundle formation. The anodized Ti grid had comparatively longer and well-defined nanotubes, which are stable, well-adherent to the grid substrate with a tube length of 1.9 ± 0.1 μm. Comparatively, 1.5 h and 1 h anodization does not show any bundle formation, yet, 1 h anodization showed shorter

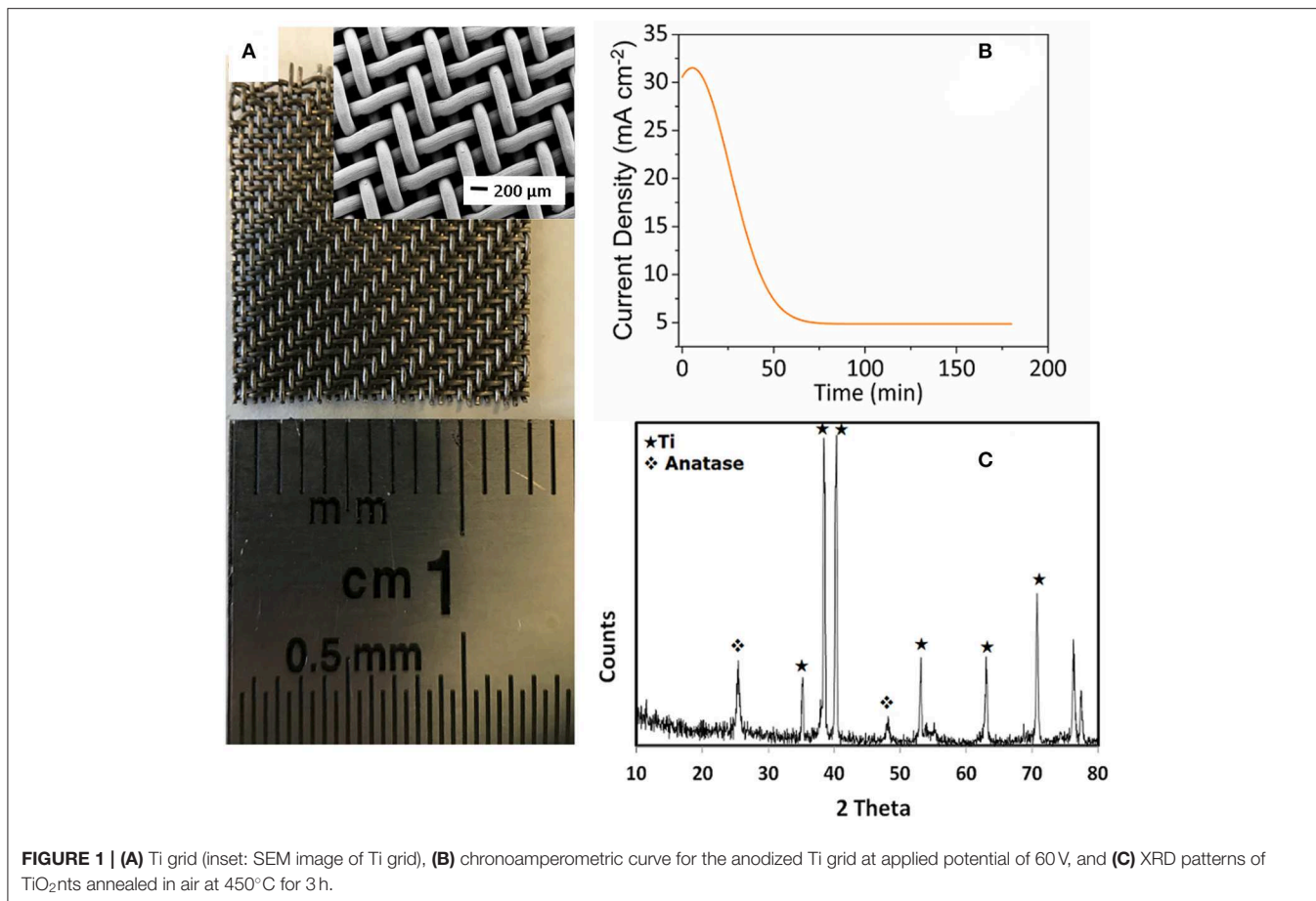
nanotubes than 1.5 h anodization. Indeed the collapse due to over dissolution of the top surface of nanotubes becomes very significant after 1.5 h. As a consequence, a substantial change in the morphology will affect the electrochemical performance of the electrodes. It is also observed that the length of the TiO<sub>2</sub>nts varies with the anodization time. The length of the TiO<sub>2</sub>nts increases as the anodization time increases from 1 to 1.5 h, afterwards the length does not continue to increase with longer anodization time.

After longer anodization time (2.5 and 3 h), the nanotubes have closed-top structure and the bundled formation is found covering the entire top surface of the nanotubes. The thickness of the nanotubes layer after 2.5 and 3 h anodization are 1.8 ± 0.2 and 1.5 ± 0.2 μm, respectively. Some studies showed that in long-duration anodization experiments, tubes can have inhomogeneous structures due to etching of the top [37]. The bundles on the tube tops might be formed due to the formation of needle-like morphologies as the walls may become too thin to support their own weight [11, 38]. This bundle morphology is also described as nanograss or nanospike [39, 40].

Nevertheless, when the anodization time is decreased, the bundle formation is disappeared. So, an appropriate oxidation time is the essential condition for the fabrication of highly ordered TiO<sub>2</sub> nanotube arrays onto Ti grid. These findings are in good agreement with the previous report. Mor et al. reported that the nanotubes can grow longer by extending the anodization time, however the top of the nanotubes are gradually destroyed after extended anodization. The partial collapse of the nanotubes occurred due to an over dissolution reaction of the tubes top during the prolonged anodization, leading to the formation of bundled nanotubes [41, 42]. Also, Zeng et al. reported that TiO<sub>2</sub> nanotubes grown on Ti grid showing a well-defined nanotubular structure after 20 min anodization, however the tubes top become fuzzy after prolonging the anodization time to 40 min [25]. Liu et al. [43] investigated the effect of the anodization time on the growth of TiO<sub>2</sub> nanotubes onto Ti grid at 60 V for 1–16 h and reported that the nanotube arrays grew uniformly after 3 h anodization. Additionally, as seen in **Figure 2**, several fissures and bundling on the surfaces of the nanotubes could also be attributed to van der Waals attraction and capillary forces during drying [11, 26, 34].

Indeed, compared to Ti foils substrate, the intertwined structure of the Ti grid had more promising results in terms of surface area. As a result, the electrolyte can penetrate easily to the entire surface of the nanotubes that are radially grown in a 3-D array on the Ti grid [43, 44]. Therefore, to further study the electrochemical performance of the self-organized TiO<sub>2</sub>nts/Ti grid, the TiO<sub>2</sub>nts/Ti grid anodized for 1.5 h was selected to be studied as anode for all-solid-state Li-ion microbatteries using PMMA-PEG polymer electrolyte.

After growing the TiO<sub>2</sub>nts on Ti grid substrate, the conformal electrodeposition of the electrolyte into nanotubes was achieved by the cyclic voltammetry (CV) technique. This approach is highly valuable to fully exploit the large surface area offered by the nanotubes through the formation of an augmented electrode/electrolyte interface [45–49]. **Figure 3** shows the cyclic



voltammogram of the electropolymerization of the polymer electrolyte on the TiO<sub>2</sub>nts. The window of the applied cathodic potential was selected between the H<sub>2</sub> bubbling and the beginning of the proton reduction [ $-1 \text{ V} < E < E(\text{H}^+/\text{H}_2) = -0.551 \text{ V vs. Ag/AgCl}$  calculated from the Nernst equation] [46]. From cyclic voltammograms (CVs), as seen in **Figure 3A**, the absolute value of the cathodic current at  $-1 \text{ V vs. Ag/AgCl}$  drops gradually with the increasing of cycles. The fading in the current can be explained by the successive deposition of the thin polymer layers that passivated the TiO<sub>2</sub>nts electrode. Additionally, the redox peaks of Ti<sup>4+</sup>/Ti<sup>3+</sup> are not observed and it is expected that there is no irreversible change in the oxidation states of Ti during the electropolymerization reaction. By using the same electrodeposition technique on the TiO<sub>2</sub>nts/Ti foil, Plylahan et al. [47] reported that after 5 cycles CV, the growth of a polymer layer occurred inside and outside of each nanotube walls. Indeed, after 10 cycles CV, the inter-tube spaces are filled with the polymer and the nanotube walls become significantly thicker compared to the sample obtained after 5 cycle of CV. After 100 cycles, the polymer fills the inter-tube spaces and coats top surfaces of the TiO<sub>2</sub>nts/Ti grid (**Figure 3B**).

The CV experiments were performed to investigate the redox potential of TiO<sub>2</sub>nts electrodes. The CV curves were

recorded at the scan rate of  $0.1 \text{ mV s}^{-1}$  between 1 and 3 V vs. Li/Li<sup>+</sup>. In **Figure 4A**, the two curves exhibit well-defined cathodic and anodic peaks at 1.75 and 1.98 V vs. Li/Li<sup>+</sup>, respectively, corresponding to lithium insertion/extraction potentials in anatase TiO<sub>2</sub>nts. The Li insertion/extraction process is reversible as seen in the unchanged shape of the CV curves upon cycling. The consecutive decrease in the absolute cathodic current indicates the slight discharge capacity fading upon cycling. **Figure 4B** shows the galvanostatic charge/discharge profiles of the anatase TiO<sub>2</sub>nts. The profiles of each sample show flat plateaus of charge at 1.77 V vs. Li/Li<sup>+</sup> and discharge 1.88 V vs. Li/Li<sup>+</sup> which are typical profiles for the anatase TiO<sub>2</sub>nts.

The cycling performance of anatase TiO<sub>2</sub>nts using the MMA-PEG500 gel electrolyte at C/10 and C/5 rates are displayed in **Figure 4C**. The areal capacities were calculated considering a density of anatase ( $4.23 \text{ g cm}^{-3}$ ), a nanotube layer thickness ( $1.8 \pm 2 \mu\text{m}$ ) and an estimated porosity of 50% [20, 36]. The cell cycled between 1 and 3 V vs. Li/Li<sup>+</sup> delivers an average capacity of  $\sim 376 \mu\text{Ah cm}^{-2}$  at C/10 and  $\sim 350 \mu\text{Ah cm}^{-2}$  at C/5. The initial charge and discharge capacities of the electrodes are 375 and 580  $\mu\text{Ah cm}^{-2}$ , corresponding to a relatively low initial coulombic efficiency of 64.7% (**Figure 4D**). A large irreversible capacity observed



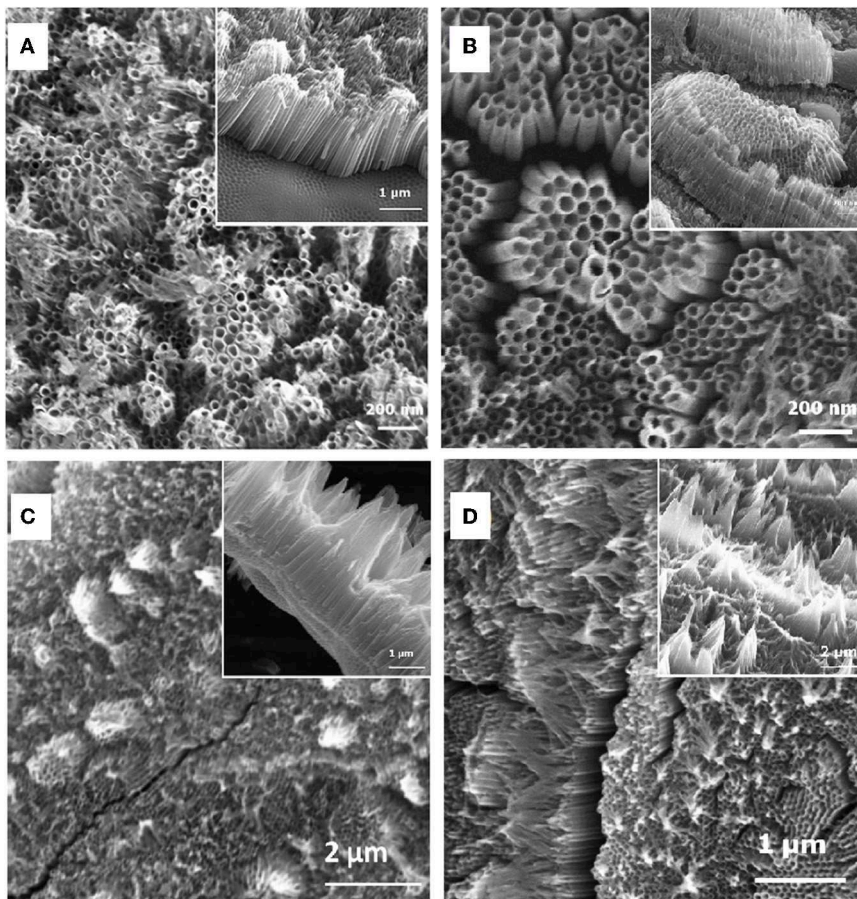


**FIGURE 2** | SEM images of TiO<sub>2</sub> nanotube arrays formed by electrochemical anodization of the Ti grid at 60 V for 1 h **(A)**, 1.5 h **(B)**, 2.5 h **(C)**, and 3 h **(D)**. Insets show the cross-sectional views.

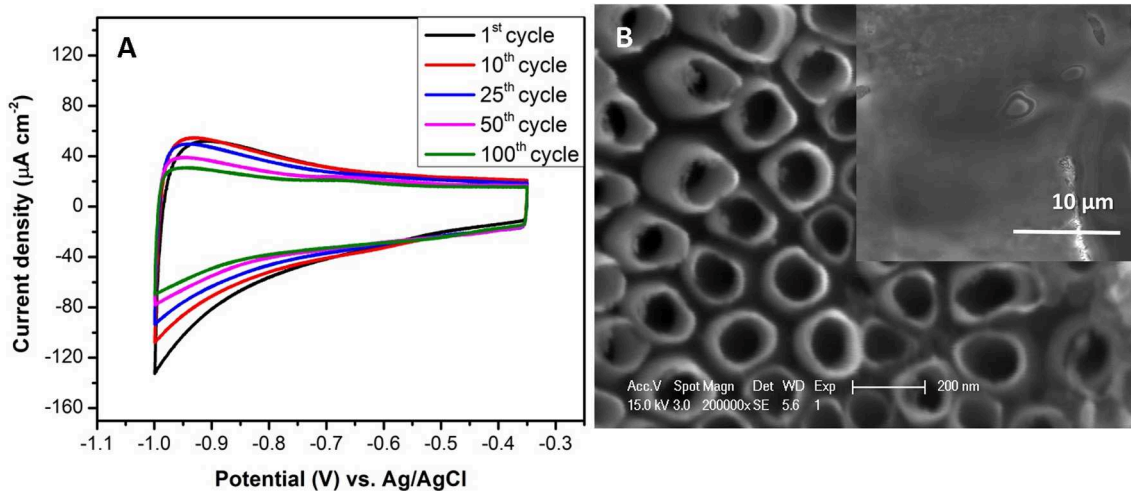


**FIGURE 3** | **(A)** Cyclic voltammograms of TiO<sub>2</sub>nts electrode in 0.5 M LiTFSI + 0.5 M MMA-PEG500. The curves were recorded in the potential window of -0.35 to -1 V vs. Ag/AgCl (3 M) at the scan rate of 10 mV s<sup>-1</sup>, **(B)** SEM images of the bare TiO<sub>2</sub>nts for 1.5 h and electropolymerized TiO<sub>2</sub>nts (inset).

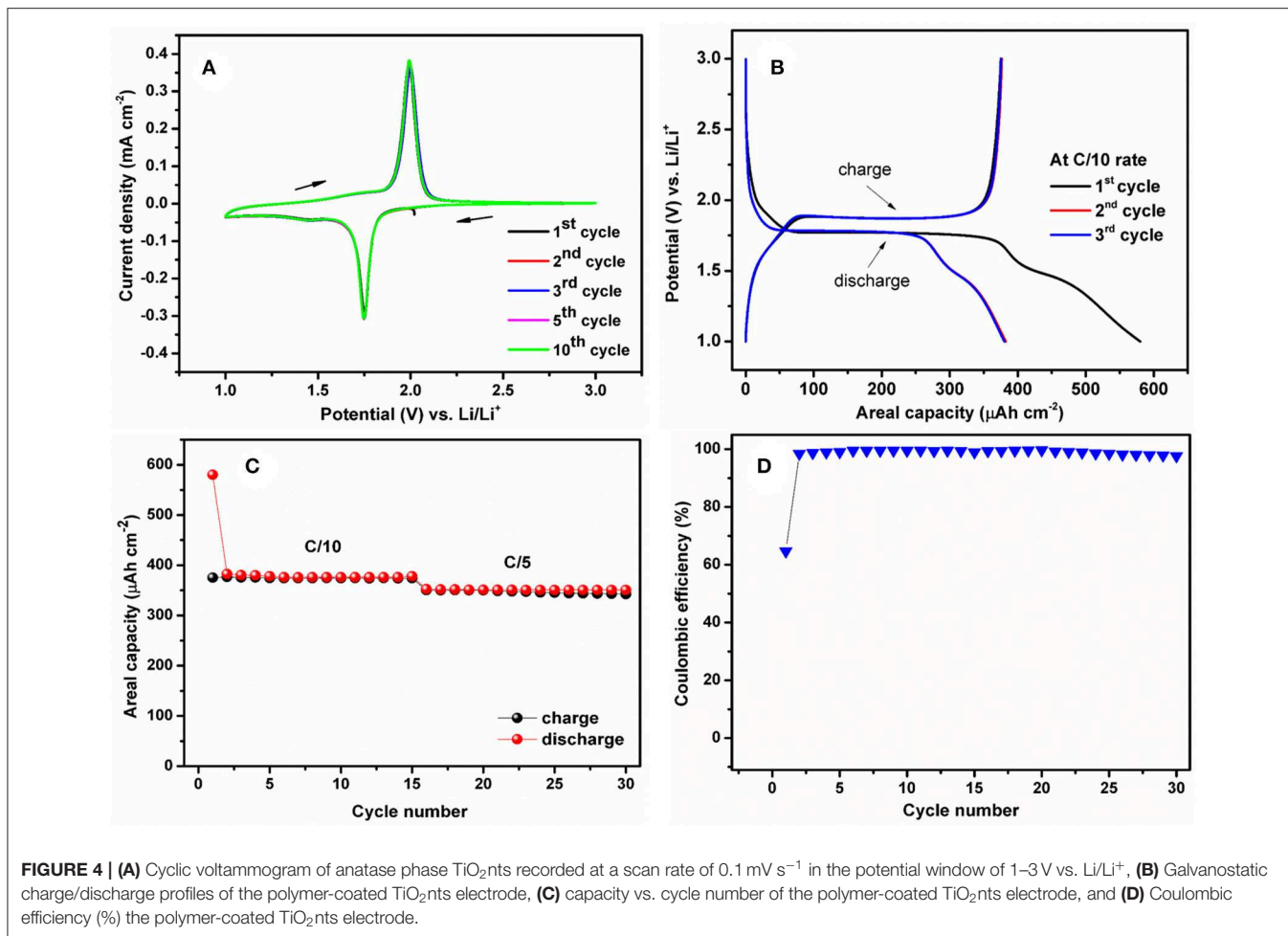


**TABLE 1 |** Electrochemical performances of the microbatteries using PMMA-PEG polymer electrolyte.

Electrodes	Areal capacity at C/10 rate after 10 cycles (μAh cm <sup>-2</sup> )	V cell (V)	Energy density (μWh cm <sup>-2</sup> )	Power density (μW cm <sup>-2</sup> )
TiO <sub>2</sub> nts/Ti foil [20]	25	1.7	43	4.3
TiO <sub>2</sub> nts/Ti grid	376	1.8	677	67.7

at the first cycles is attributed to the side reaction of Li<sup>+</sup> and the presence of residual water at the surface of TiO<sub>2</sub>nts and in the polymer electrolyte. Additionally, some Li ions are trapped inside the TiO<sub>2</sub> lattice structure after the first Li<sup>+</sup> insertion, thereby reducing the capacity of the cell [35, 50]. Nevertheless, for the subsequent cycles the capacities can be stabilized, the discharge capacity values recorded in the 2nd and 3rd cycles are 382 and 380 μAh cm<sup>-2</sup> with improved coulombic efficiency of 98.4 and 98.7%, respectively. The cycling retention continuously enhanced after first cycle and the coulombic efficiency approaches 100%.

The electrochemical performances of TiO<sub>2</sub>nts grown on Ti grid and Ti foil are summarized in **Table 1**. After 10 cycles, the storage capacity of the TiO<sub>2</sub>nts/Ti grid is 15 times higher compared to our previous report with Ti foils [14]. Calculated

using a microbattery voltage of 1.8 V, the obtained areal energy and power density of the TiO<sub>2</sub>nts/Ti grid anode are 677 μWh cm<sup>-2</sup> and 67.7 μW cm<sup>-2</sup>, respectively.

## CONCLUSION

To sum up, Ti grid is used as a 3D substrate to form self-organized TiO<sub>2</sub> nanotubes. The anodization time shows a significant influence on the morphological properties of the nanotubes. Well-defined nanotubes without bundle formation with a tube length of 1.9 ± 0.1 μm can be obtained after 1.5 h anodizing a Ti grid. Due to its radial and intertwined structure, Ti grid supplies much larger area than a Ti foil for a same footprint area. Actually, Ti grid showed much higher areal capacity in comparison to Ti

foil at the same kinetics (C/10 and C/5). The main reason is because self-supported nanotubes are successfully formed within a very large surface area increasing the amount of the active material and the battery performance. After 10 cycles, the storage capacity of the TiO<sub>2</sub>nts/Ti grid is 15 times higher compared to our previous report with Ti foils.

## DATA AVAILABILITY STATEMENT

The datasets generated for this study are available on request to the corresponding author.

## REFERENCES

1. Baggetto L, Knoop HCM, Niessen RAH, Kessels WMM, Notten PHL. 3D negative electrode stacks for integrated all-solid-state lithium-ion microbatteries. *J Mater Chem.* (2010) **20**:3703–8. doi: 10.1039/b926044g
2. Armand M, Tarascon J-M. Building better batteries. *Nature.* (2008) **451**:652–7. doi: 10.1038/451652a
3. Sugawati VA, Vacandio F, Eyraud M, Knauth P, Djenizian T. Porous NASICON-type Li<sub>3</sub>Fe<sub>2</sub>(PO<sub>4</sub>)<sub>3</sub> thin film deposited by RF sputtering as cathode material for Li-ion microbatteries. *Nanoscale Res Lett.* (2016) **11**:365. doi: 10.1186/s11671-016-1574-7
4. Sugawati VA, Vacandio F, Knauth P, Djenizian T. Sputter-deposited amorphous LiCuPO<sub>4</sub> thin film as cathode material for Li-ion microbatteries. *ChemistrySelect.* (2018) **3**:405–9. doi: 10.1002/slct.201702429
5. Ferrari S, Loveridge M, Beattie SD, Jahn M, Dashwood RJ, Bhagat R. Latest advances in the manufacturing of 3D rechargeable lithium microbatteries. *J Power Sources.* (2015) **286**:25–46. doi: 10.1016/j.jpowsour.2015.03.133
6. Nasreldin M, Delattre R, Ramuz M, Lahuc C, Djenizian T, de Bougrenet de la Tocnaye J-L. Flexible micro-battery for powering smart contact lens. *Sensors.* (2019) **19**:2062. doi: 10.3390/s19092062
7. Zheng S, Wu Z-S, Zhou F, Wang X, Ma J, Liu C, et al. All-solid-state planar integrated lithium ion micro-batteries with extraordinary flexibility and high-temperature performance. *Nano Energy.* (2018) **51**:613–20. doi: 10.1016/j.nanoen.2018.07.009
8. Oudenhoven JFM, Baggetto L, Notten PHL. All-solid-state lithium-ion microbatteries: a review of various three-dimensional concepts. *Adv Energy Mater.* (2011) **1**:10–33. doi: 10.1002/aenm.201000002
9. Jaroenworalluck A, Regonini D, Bowen CR, Stevens R, Allsopp D. Macro, micro and nanostructure of TiO<sub>2</sub> anodized films prepared in a fluorine-containing electrolyte. *J Mater Sci.* (2007) **42**:6729–34. doi: 10.1007/s10853-006-1474-9
10. Fraoucene H, Sugawati VA, Hatem D, Belkaid MS, Vacandio F, Eyraud M, et al. Optical and electrochemical properties of self-organized TiO<sub>2</sub> nanotube arrays from anodized Ti–6Al–4V alloy. *Front Chem.* (2019) **7**:66. doi: 10.3389/fchem.2019.00066
11. Roy P, Berger S, Schmuki P. TiO<sub>2</sub> nanotubes: synthesis and applications. *Angew Chem Int Ed.* (2011) **50**:2904–39. doi: 10.1002/anie.201001374
12. Krysa J, Lee K, Pausova S, Kment S, Hubicka Z, Cvrtilik R, et al. Self-organized transparent 1D TiO<sub>2</sub> nanotubular photoelectrodes grown by anodization of sputtered and evaporated Ti layers: a comparative photoelectrochemical study. *Chem Eng J.* (2017) **308**:745–53. doi: 10.1016/j.cej.2016.09.112
13. Galstyan V, Vomiero A, Comini E, Faglia G, Sberveglieri G. TiO<sub>2</sub> nanotubular and nanoporous arrays by electrochemical anodization on different substrates. *RSC Adv.* (2011) **1**:1038–44. doi: 10.1039/c1ra00077b
14. Assafpour-Dezfuly M, Vlachos C, Andrews EH. Oxide morphology and adhesive bonding on titanium surfaces. *J Mater Sci.* (1984) **19**:3626–39. doi: 10.1007/BF00552275
15. Zwilling V, Darque-Ceretti E, Boutry-Forveille A, David D, Perrin MY, Accouturier M. Structure and physicochemistry of anodic oxide films on titanium and TA6V alloy. *Surf Interface Anal.* (1999) **27**:629–37. doi: 10.1002/(SICI)1096-9918(199907)27:7<629::AID-SIA551>3.0.CO;2-0
16. Zhou X, Liu N, Schmuki P. Photocatalysis with TiO<sub>2</sub> nanotubes: “Colorful” reactivity and designing site-specific photocatalytic centers into TiO<sub>2</sub> nanotubes. *ACS Catal.* (2017) **7**:3210–35. doi: 10.1021/acscatal.6b03709
17. Galstyan V, Comini E, Baratto C, Ferroni M, Poli N, Faglia G, et al. Two-phase titania nanotubes for gas sensing. *Procedia Eng.* (2014) **87**:176–9. doi: 10.1016/j.proeng.2014.11.612
18. Shankar K, Mor GK, Prakasam HE, Varghese OK, Grimes CA. Self-assembled hybrid polymer–TiO<sub>2</sub> nanotube array heterojunction solar cells. *Langmuir.* (2007) **23**:12445–9. doi: 10.1021/la7020403
19. Ellis BL, Knauth P, Djenizian T. Three-dimensional self-supported metal oxides for advanced energy storage. *Adv Mater.* (2014) **26**:3368–97. doi: 10.1002/adma.201306126
20. Plylahan N, Letiche M, Samy Barr MK, Ellis B, Maria S, Phan TNT, et al. High energy and power density TiO<sub>2</sub> nanotube electrodes for single and complete lithium-ion batteries. *J Power Sources.* (2015) **273**:1182–8. doi: 10.1016/j.jpowsour.2014.09.152
21. Macák JM, Tsuchiya H, Schmuki P. High-aspect-ratio TiO<sub>2</sub> nanotubes by anodization of titanium. *Angew Chem Int Ed.* (2005) **44**:2100–2. doi: 10.1002/anie.200462459
22. Sopha H, Salián GD, Zazpe R, Prikryl J, Hromadko L, Djenizian T, et al. ALD Al<sub>2</sub>O<sub>3</sub>-coated TiO<sub>2</sub> nanotube layers as anodes for lithium-ion batteries. *ACS Omega.* (2017) **2**:2749–56. doi: 10.1021/acsomega.7b00463
23. Salián GD, Krbal M, Sopha H, Lebouin C, Coulet M-V, Michalicka J, et al. Self-supported sulphurized TiO<sub>2</sub> nanotube layers as positive electrodes for lithium microbatteries. *Appl Mater Today.* (2019) **16**:257–64. doi: 10.1016/j.apmt.2019.05.015
24. Salián GD, Koo BM, Lefevre C, Cottineau T, Lebouin C, Tesfaye AT, et al. Niobium alloying of self-organized TiO<sub>2</sub> nanotubes as an anode for lithium-ion microbatteries. *Adv Mater Technol.* (2018) **3**:1700274. doi: 10.1002/admt.201700274
25. Zeng Q-Y, Xi M, Xu W, Li X-J. Preparation of titanium dioxide nanotube arrays on titanium mesh by anodization in (NH<sub>4</sub>)<sub>2</sub>SO<sub>4</sub>/NH<sub>4</sub>F electrolyte. *Mater Corros.* (2013) **64**:1001–6. doi: 10.1002/maco.201106481
26. Gulati K, Santos A, Findlay D, Losic D. Optimizing anodization conditions for the growth of titania nanotubes on curved surfaces. *J Phys Chem C.* (2015) **119**:16033–45. doi: 10.1021/acs.jpcc.5b03383
27. He W, Qiu J, Zhuge F, Li X, Lee J-H, Kim Y-D, et al. Advantages of using Ti-mesh type electrodes for flexible dye-sensitized solar cells. *Nanotechnology.* (2012) **23**:225602. doi: 10.1088/0957-4484/23/22/225602
28. Chun KY, Park BW, Sung YM, Kwak DJ, Hyun YT, Park MW. Fabrication of dye-sensitized solar cells using TiO<sub>2</sub>-nanotube arrays on Ti-grid substrates. *Thin Solid Films.* (2009) **517**:4196–8. doi: 10.1016/j.tsf.2009.02.042
29. Gerosa M, Sacco A, Scalia A, Bella F, Chiodoni A, Quaglio M, et al. Toward totally flexible dye-sensitized solar cells based on titanium grids and polymeric electrolyte. *IEEE J Photovolt.* (2016) **6**:498–505. doi: 10.1109/JPHOTOV.2016.2514702
30. Liu Z, Subramania V (Ravi), Misra M. Vertically oriented TiO<sub>2</sub> nanotube arrays grown on Ti meshes for flexible dye-sensitized solar cells. *J Phys Chem C.* (2009) **113**:14028–33. doi: 10.1021/jp903342s
31. Motola M, Dworniczek E, Satrapinsky L, Chodaczek G, Grzesiak J, Gregor M, et al. UV light-induced photocatalytic, antimicrobial, and

## AUTHOR CONTRIBUTIONS

VS performed experiments, analyzed the experimental results, and wrote the manuscript. VS, AG, AK, FV, and TD discussed experimental results. FV and TD supervised the works. All the authors contributed to the reading of paper and gave advice on the revision of the manuscript.

## ACKNOWLEDGMENTS

We acknowledge Région Sud for the financial support.

- antibiofilm performance of anodic TiO<sub>2</sub> nanotube layers prepared on titanium mesh and Ti sputtered on silicon. *Chem Pap.* (2019) **73**:1163–72. doi: 10.1007/s11696-018-0667-4
32. Martin M, Leonid S, Tomáš R, Jan Š, Jaroslav K, Mariana K, et al. Anatase TiO<sub>2</sub> nanotube arrays and titania films on titanium mesh for photocatalytic NOX removal and water cleaning. *Catal Today.* (2017) **287**:59–64. doi: 10.1016/j.cattod.2016.10.011
33. Rustomji CS, Frandsen CJ, Jin S, Tauber MJ. Dye-sensitized solar cell constructed with titanium mesh and 3-D array of TiO<sub>2</sub> nanotubes. *J Phys Chem B.* (2010) **114**:14537–43. doi: 10.1021/jp102299g
34. Liao J, Lin S, Zhang L, Pan N, Cao X, Li J. Photocatalytic degradation of methyl orange using a TiO<sub>2</sub>/Ti mesh electrode with 3D nanotube arrays. *ACS Appl Mater Interfaces.* (2012) **4**:171–7. doi: 10.1021/am201220e
35. Ozkan S, Nguyen NT, Mazare A, Cerri I, Schmuki P. Controlled spacing of self-organized anodic TiO<sub>2</sub> nanotubes. *Electrochem Commun.* (2016) **69**:76–9. doi: 10.1016/j.elecom.2016.06.004
36. Plylahan N, Letiche M, Barr MKS, Djenizian T. All-solid-state lithium-ion batteries based on self-supported titania nanotubes. *Electrochem Commun.* (2014) **43**:121–4. doi: 10.1016/j.elecom.2014.03.029
37. Macak JM, Tsuchiya H, Taveira L, Aldabergerova S, Schmuki P. Smooth anodic TiO<sub>2</sub> nanotubes. *Angew Chem Int Ed.* (2005) **44**:7463–5. doi: 10.1002/anie.200502781
38. Macak JM, Schmuki P. Anodic growth of self-organized anodic TiO<sub>2</sub> nanotubes in viscous electrolytes. *Electrochim Acta.* (2006) **52**:1258–64. doi: 10.1016/j.electacta.2006.07.021
39. Song Y-Y, Lynch R, Kim D, Roy P, Schmuki P. TiO<sub>2</sub> nanotubes: efficient suppression of top etching during anodic growth key to improved high aspect ratio geometries. *Electrochem Solid State Lett.* (2009) **12**:C17–20. doi: 10.1149/1.3126500
40. Kirchgeorg R, Kallert M, Liu N, Hahn R, Killian MS, Schmuki P. Key factors for an improved lithium ion storage capacity of anodic TiO<sub>2</sub> nanotubes. *Electrochim Acta.* (2016) **198**:56–65. doi: 10.1016/j.electacta.2016.03.009
41. Mor GK, Varghese OK, Paulose M, Shankar K, Grimes CA. A review on highly ordered, vertically oriented TiO<sub>2</sub> nanotube arrays: fabrication, material properties, and solar energy applications. *Solar Energy Mater Solar Cells.* (2006) **90**:2011–75. doi: 10.1016/j.solmat.2006.04.007
42. Altomare M, Pozzi M, Allieta M, Bettini LG, Selli E. H<sub>2</sub> and O<sub>2</sub> photocatalytic production on TiO<sub>2</sub> nanotube arrays: effect of the anodization time on structural features and photoactivity. *Appl Catal B Environ.* (2013) **136–137**:81–8. doi: 10.1016/j.apcatb.2013.01.054
43. Liu Z, Zhang Q, Zhao T, Zhai J, Jiang L. 3-D vertical arrays of TiO<sub>2</sub> nanotubes on Ti meshes: efficient photoanodes for water photoelectrolysis. *J Mater Chem.* (2011) **21**:10354–8. doi: 10.1039/c1jm11072a
44. Zhang Z-J, Zeng Q-Y, Chou S-L, Li X-J, Li H-J, Ozawa K, et al. Tuning three-dimensional TiO<sub>2</sub> nanotube electrode to achieve high utilization of Ti substrate for lithium storage. *Electrochim Acta.* (2014) **133**:570–7. doi: 10.1016/j.electacta.2014.04.049
45. Ferrari IV, Braglia M, Djenizian T, Knauth P, Di Vona ML. Electrochemically engineered single Li-ion conducting solid polymer electrolyte on titania nanotubes for microbatteries. *J Power Sources.* (2017) **353**:95–103. doi: 10.1016/j.jpowsour.2017.03.141
46. Salian GD, Lebouin C, Demoulin A, Lepihin MS, Maria S, Galeyeva AK, et al. Electrodeposition of polymer electrolyte in nanostructured electrodes for enhanced electrochemical performance of thin-film Li-ion microbatteries. *J Power Sources.* (2017) **340**:242–6. doi: 10.1016/j.jpowsour.2016.11.078
47. Plylahan N, Maria S, Phan TN, Letiche M, Martinez H, Courrèges C, et al. Enhanced electrochemical performance of Lithium-ion batteries by conformal coating of polymer electrolyte. *Nanoscale Res Lett.* (2014) **9**:544. doi: 10.1186/1556-276X-9-544
48. Sugiyawati VA, Vacandio F, Ein-Eli Y, Djenizian T. Electrodeposition of polymer electrolyte into carbon nanotube tissues for high performance flexible Li-ion microbatteries. *APL Mater.* (2019) **7**:031506. doi: 10.1063/1.5082837
49. Braglia M, Ferrari IV, Djenizian T, Kaciulis S, Soltani P, Di Vona ML, et al. Bottom-up electrochemical deposition of poly(styrene sulfonate) on nanoarchitected electrodes. *ACS Appl Mater Interfaces.* (2017) **9**:22902–10. doi: 10.1021/acsami.7b04335
50. Ortiz GF, Hanzu I, Djenizian T, Lavela P, Tirado JL, Knauth P. Alternative Li-ion battery electrode based on self-organized titania nanotubes. *Chem Mater.* (2009) **21**:63–7. doi: 10.1021/cm801670u

**Conflict of Interest:** The authors declare that the research was conducted in the absence of any commercial or financial relationships that could be construed as a potential conflict of interest.

Copyright © 2019 Sugiyawati, Vacandio, Galeyeva, Kurbatov and Djenizian. This is an open-access article distributed under the terms of the Creative Commons Attribution License (CC BY). The use, distribution or reproduction in other forums is permitted, provided the original author(s) and the copyright owner(s) are credited and that the original publication in this journal is cited, in accordance with accepted academic practice. No use, distribution or reproduction is permitted which does not comply with these terms.